

Acquiring higher lumen efficacy and color rendering index with green $\text{NaYF}_4:\text{Er}^{3+}\text{Yb}^{3+}$ and red $\alpha\text{-SrO}\cdot 3\text{B}_2\text{O}_3:\text{Sm}^{2+}$ layers for designing remote phosphor LED

My Hanh Nguyen Thi¹, Nguyen Thi Phuong Loan², Nguyen Doan Quoc Anh³

¹Faculty of Mechanical Engineering, Industrial University of Ho Chi Minh City, Vietnam

²Faculty of Fundamental 2, Posts and Telecommunications Institute of Technology, Vietnam

³Power System Optimization Research Group, Faculty of Electrical and Electronics Engineering, Ton Duc Thang University, Vietnam

Article Info

Article history:

Received Aug 3, 2019

Revised Jun 30, 2020

Accepted Jul 9, 2020

Keywords:

Color rendering index

Lumen output

$\text{NaYF}_4:\text{Er}^{3+}\text{Yb}^{3+}$

WLEDs

$\alpha\text{-SrO}\cdot 3\text{B}_2\text{O}_3:\text{Sm}^{2+}$

ABSTRACT

Lighting devices that apply diodes to create white light-emitting diodes (WLEDs) can achieve remarkable results in color quality, especially those containing quantum dots (QDs) and phosphor. The technique to create an appropriate package is providing spaces between the QDs and phosphor components which helps decrease the ratio of the reabsorption losses and keeps the QDs surface ligands constant. The research aims to perfect the constructing method of remote phosphor configuration containing quantum dots and phosphor materials that based on lighting properties and temperature feature of WLEDs. The infrared thermography is the tool to measure and analyze total emitted light and emission ranges of the device. This device is also used in temperature simulation and experimental verification. At the given mA of 60, the WLEDs structure with green QDs layer above the phosphor layer results in 996 lm luminous flux (LF), and $R_a = 57$ in color rendering ability. Meanwhile, luminous flux of WLEDs with red QDs-on-phosphor structure is 632, and $R_a = 70$. Furthermore, comparing with the green QDs-on-phosphor type, the red QDs-on-phosphor type emitted less LF. However, the red QDs-on-phosphor type can be the most effective package design to achieve color rendering ability.

This is an open access article under the [CC BY-SA](https://creativecommons.org/licenses/by-sa/4.0/) license.



Corresponding Author:

Nguyen Doan Quoc Anh,
Power System Optimization Research Group,
Faculty of Electrical and Electronics Engineering,
Ton Duc Thang University,
Ho Chi Minh City, Vietnam.
Email: nguyendoanquocanh@tdtu.edu.vn

1. INTRODUCTION

As solid-state lighting (SSL) sources become more and more popular in both indoor and outdoor applications, there are many lighting devices fabricated to meet the demands in the modern illumination market. Among various invented lighting devices, light-emitting diodes that generate energy from phosphor (pc-LEDs) are the most popular lighting solution for superior characteristics in luminescence efficacy, power savings, and endurance [1-3]. Pc-LEDs package is usually a structure containing light emitting chips and the phosphor substance $\text{Y}_3\text{Al}_5\text{O}_{12}:\text{Ce}^{3+}$ (YAG:Ce). In this structure, the phosphor layer absorbs a proportion of the blue light from LED chips, and then the lights are converted into yellow lights. After that, white light is generated as a result

of combination between the emitted light from the chips and phosphor. This method provide LEDs with high lighting efficacy, but the low color quality caused by the lack of color red in the spectrum is a problem [4]. Hence, the enhancement of color rendering abilities of pc-LEDs becomes so important that take plenty of efforts from researchers to figure out the best method. There are many approaches have been proposed and adding red phosphors with high efficiency emission is one of them [5-8]. Nevertheless, the large emission of the red phosphor is not fully compatible with the sensitive zone of human eyes, leading to its ineffectiveness in generating the high lighting efficacy (LE) [9]. In terms of producing the white light-emitting diodes (WLEDs) having high luminous output and color rendering index (CRI) for SSL applications, semiconductor such as quantum dots (QDs) has all the qualities that both researchers and manufacturers need.

Their exceptional qualities such as small light discharge range, adjustable bandwidth and great quantum efficiency [10-13], are confirmed to have a great impact on WLEDs performance. Many researches and experiments have been conducted and confirmed that adding quantum material in LEDs devices enhances CRI and color quality while letting LE retained its high value due to the QDs' narrow emission [14-16]. For the method to install QDs into pc-LEDs, there are two ways suggested. The first one is mixing QDs and phosphor-silicone gel and put them over the LED chips' surface, such as the mixed structure [17, 18]. In this design, the reflection cup is filled with the QDs and placed closely to the LED chip, leading to the high optical energy density pressing on QDs. The second approach is seperating the QDs and phosphor materials, similar to the phosphor layers in remote pc-LEDs package [19, 20]. The QDs film will be placed far from the LED chip, and as a result, the optical power density has little effect on the QDs. Moreover, the chemical compatibility of QDs surface ligands and phosphor compound in the remote design are more flexible because of QDs' adjustable polymeric condition [21, 22]. For those reasons, the remote structure compositing of both QDs and phosphor layer become the optimal approach to produce the high-quality WLEDs with superior luminous flux (LF) and CRI.

2. PREPARATION AND SIMULATION

Figure 1 illustrated the constructions of WLEDs with QDs and phosphor layer. In Figure 1 (a), the structure called type I has the green QDs layer placed over the phosphor layer. On the other hand, type II WLEDs is designed in the opposite way with red QDs layer covers the phosphor material beneath, as illustrated by Figure 1 (b). The arrangement of phosphor and QDs material is a deciding factor of LEDs light output because it affect thermal distribution, and then bring the difference to the long-term stability. The relation of QDs and phosphor materials with the overall performance of lighting devices have been investigated and discussed in various studies, however, one important aspect which is the transmitting light energy between these materials was not specifically analyzed. Yet, the drawbacks of these types were not discovered at that time. In fact, there is a loss in energy power transferring between QDs and phosphor existing. Moreover, the QDs is not constant and their effects on different outputs of WLEDs have not been taken into account. Thus, this research paper carried out a quantitative analysis of performance variation of the two QDs-WLEDs structures. The research team has performed calculations to estimate the loss of emitted light power from both constituent materials for analyzation. Besides, the fabrication CdSe/ZnS quantum dots that emits red chromatic light was carried out with the result being applied to the YAG:Ce phosphor layer and different QDs films to manufacture WLEDs. The sphere system was integrated into the structure to measure and analyze the output optical power and PL spectra. The combination between optical measurement and thermal simulation is applied to simulate the temperature zones which is verified by infrared thermal camera. Finally, the results indicated that the QDs-on-phosphor type can enhance the lighting devices in light output, CRI, and thermal performance.

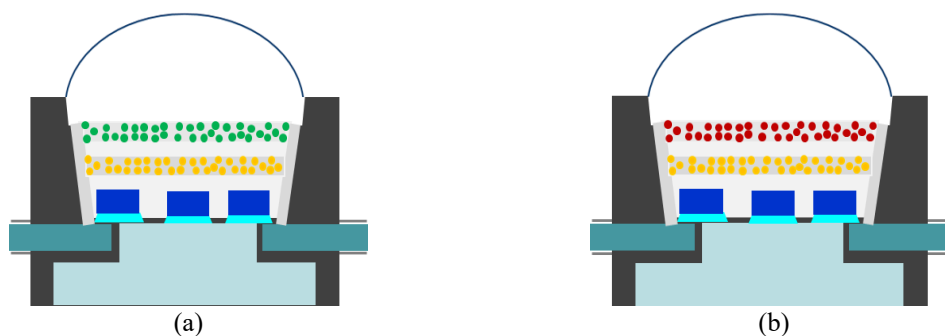


Figure 1. The illustration of the two-remote type WLEDs with different designs; (a) green QDs-on-phosphor type, (b) red QDs-on-phosphor type

3. RESULTS AND DISCUSSION

The change in concentration among the three phosphors green $\text{NaYF}_4:\text{Er}^{3+}, \text{Yb}^{3+}$, red $\alpha\text{-SrO}\cdot 3\text{B}_2\text{O}_3:\text{Sm}^{2+}$, and yellow $\text{YAG}:\text{Ce}^{3+}$ is incompatible, as demonstrated in Figure 2. The adjustment of these phosphors' concentrations is to achieve the two purposes. The first one is to keep the ACCTs and the second one is to change the scattering and absorbing abilities of the phosphor layers inside WLEDs for higher color quality and lumen output. Therefore, it is vital to choose the appropriate values for the concentration of $\text{NaYF}_4:\text{Er}^{3+}, \text{Yb}^{3+}$ and $\alpha\text{-SrO}\cdot 3\text{B}_2\text{O}_3:\text{Sm}^{2+}$ if the manufacturers want to improve chromatic quality of WLEDs. On the other hand, as the $\text{NaYF}_4:\text{Er}^{3+}, \text{Yb}^{3+}$ and $\alpha\text{-SrO}\cdot 3\text{B}_2\text{O}_3:\text{Sm}^{2+}$ concentrations increase from 2 to 20%, $\text{YAG}:\text{Ce}^{3+}$ must decline to stabilize the ACCTs. This modification is made to balance the proportions of primary color materials in lighting devices and prevent damages to color quality.

Obviously, red phosphor $\alpha\text{-SrO}\cdot 3\text{B}_2\text{O}_3:\text{Sm}^{2+}$ being added to the structure bring many changes to the emission spectrum of WLEDs, according to Figure 3. Thus, based on the purpose of manufacturer, the suitable amount of it is determined. As the main requirement for producing WLEDs is its color quality, a small decrease in lumen output is acceptable. For this requirement, utilizing the green $\text{NaYF}_4:\text{Er}^{3+}, \text{Yb}^{3+}$ phosphor in the structure comes with impressive results. As can be seen, green phosphor $\text{NaYF}_4:\text{Er}^{3+}, \text{Yb}^{3+}$ increases in volume widens the emission spectrum in the wavelength bands of 420-480 nm and 500-640 nm. This growth exhibits that the luminous flux also increases. Additionally, the rise of internal blue-light scattering of WLEDs means that the scattering occurring in phosphor layer and WLEDs is raised, and this is beneficial to the correlated color. For red $\alpha\text{-SrO}\cdot 3\text{B}_2\text{O}_3:\text{Sm}^{2+}$, as the amount of phosphor increases, emission spectrum intensity of red light in the range of 648-738 nm rises. However, in the ranges of 420-480 nm and 500-640 nm, $\alpha\text{-SrO}\cdot 3\text{B}_2\text{O}_3:\text{Sm}^{2+}$ does not give the same qualified result as $\text{NaYF}_4:\text{Er}^{3+}, \text{Yb}^{3+}$. Hence, the scattering in the red phosphor layer is not improve because the scattered blue light is the result of light emission in between 420 nm and 480 nm wavelengths. Furthermore, there is a noticeable result from applying the red phosphor $\alpha\text{-SrO}\cdot 3\text{B}_2\text{O}_3:\text{Sm}^{2+}$. When there is a higher temperature, the emission spectrum is also lifted, and as a result, the chromatic quality and lumen efficiency are also improved. Meanwhile, achieving the high color quality in WLEDs with high ACCTs is considered as a tough task to fulfill. Therefore, the article assures that red-emitting phosphor benefits color quality of WLEDs with any ACCTs.

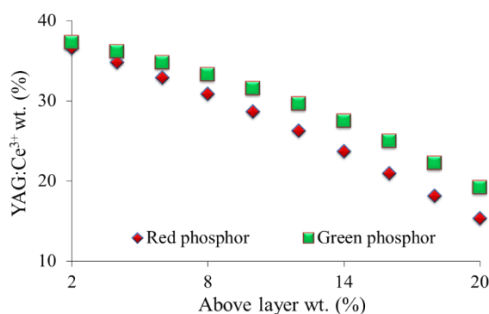


Figure 2. The modification of concentrations among the three phosphors yellow, red and green in maintaining the ACCT

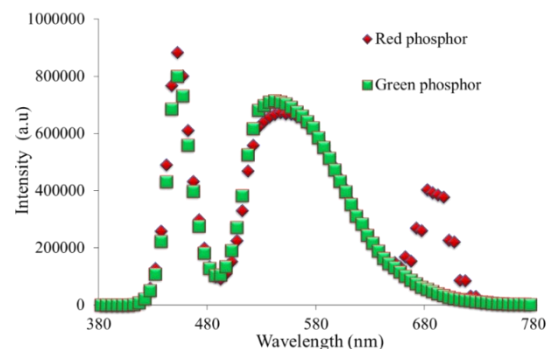


Figure 3. Emission spectra of dual-layer phosphor configurations with red and green phosphor layers

The color rendering ability of a lighting device indicates the proficiency in expressing the chromatic traits of entities under its light often denoted as CRI, and this parameter can be affected by the lighting temperature. Moreover, the discrepancy between primary colors forming white light caused by redundant green light component, also decrease the color quality as well as the accuracy of WLEDs color. Figure 4 exhibits the slight downward fluctuation of CRI with the presence of the green phosphor layer $\text{NaYF}_4:\text{Er}^{3+}, \text{Yb}^{3+}$. Nonetheless, the CRI does not fully evaluate the color quality of WLEDs, therefore this slight decline is acceptable. Besides, due to the inability of CRI to assess certain aspects of light quality, another parameter such as color quality scale (CQS) stands out as a better fit. This quality indicator is deemed more comprehensive than CRI because it can distinguish the color quality of light without any disparity, based on the combination of CRI, the viewer's preference and the color coordinates. These criteria show that CQS holds greater values than CRI, therefore, accomplishing high CQS is a more important priority to CRI. Observing the CQS results presented in Figure 5 which show CQS remains stable when the $\text{NaYF}_4:\text{Er}^{3+}, \text{Yb}^{3+}$ concentration does not increase over 8%. Hence, the appropriate amount of $\text{NaYF}_4:\text{Er}^{3+}, \text{Yb}^{3+}$ concentration for better color quality is 8%.

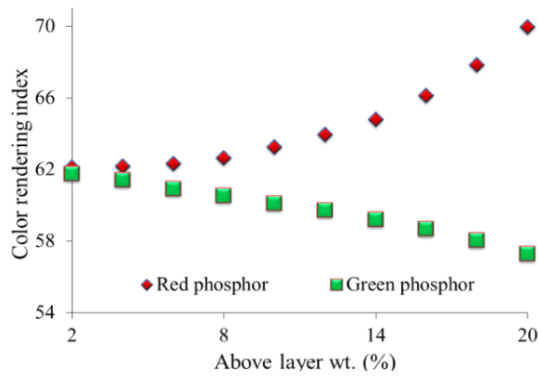


Figure 4. The color rendering index in connection with the variation of NaYF₄:Er³⁺, Yb³⁺ and α-SrO·3B₂O₃:Sm²⁺ phosphors' concentration

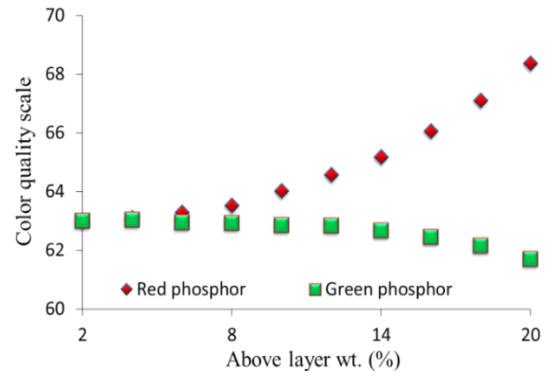


Figure 5. The color quality scale in connection with the variation of NaYF₄:Er³⁺, Yb³⁺ and α-SrO·3B₂O₃:Sm²⁺ phosphors' concentration

This part demonstrates the mathematics system of the spectral power distribution (SPD) of WLEDs with YAG phosphor coating. The Gaussian function is used to form the mathematics equation of the asymmetric SPD of monochrome LED [23-25]. The SPD (mW/nm) can be expressed as:

$$P_{\lambda} = P_{opt} \frac{1}{\sigma\sqrt{2\pi}} \exp \left[-0.5 * \frac{(\lambda - \lambda_{peak})^2}{\sigma^2} \right] \tag{1}$$

in which, P_{opt} is the optical power, and σ is affected by peak wavelength λ_{peak} . Meanwhile, the full-width at half-maximum (FWHM) $\Delta\lambda$ can be defined as:

$$\sigma = \frac{\lambda_{peak}^2 \Delta E}{2hc\sqrt{2} \ln 2} = \frac{\lambda_{peak}^2 (\frac{hc}{\lambda_1} - \frac{hc}{\lambda_2})}{2hc\sqrt{2} \ln 2} = \frac{\lambda_{peak}^2 (\frac{hc\Delta\lambda}{\lambda_1\lambda_2})}{2hc\sqrt{2} \ln 2} \tag{2}$$

where h is the planck's constant, c presents the speed of light, and the parameters λ_1 and λ_2 are the wavelengths at half of the peak intensity. In the theoretical angle, the SPD of a WLEDs with YAG phosphor coating and blue LED chip can be viewed as a spectral combination between blue and yellow light. The yellow phosphor, in reality, capable of light emission at both blue and green emission spectra, therefore, green spectrum is applicable in exhibiting the discrepancy of the realistic SPD in comparison to the selected model combining only blue and yellow light emitting ranges. Hence, to accurately depict the actual result, green spectrum is added to the calculation model of optical power in bi-color configuration. The final model is the spectrum model with three colors (blue, green, yellow) as expressed in (3) and then revised in (4):

$$P_{\lambda} = P_{opt_b} \frac{1}{\sigma_b\sqrt{2\pi}} \exp \left[-0.5 * \frac{(\lambda - \lambda_{peak_b})^2}{\sigma_b^2} \right] + P_{opt_g} \frac{1}{\sigma_g\sqrt{2\pi}} \exp \left[-0.5 * \frac{(\lambda - \lambda_{peak_g})^2}{\sigma_g^2} \right] + P_{opt_y} \frac{1}{\sigma_y\sqrt{2\pi}} \exp \left[-0.5 * \frac{(\lambda - \lambda_{peak_y})^2}{\sigma_y^2} \right] \tag{3}$$

$$P_{\lambda} = \eta_b P_{opt_total} \frac{1}{\sigma_b\sqrt{2\pi}} \exp \left[-0.5 * \frac{(\lambda - \lambda_{peak_b})^2}{\sigma_b^2} \right] + \eta_g P_{opt_total} \frac{1}{\sigma_g\sqrt{2\pi}} \exp \left[-0.5 * \frac{(\lambda - \lambda_{peak_g})^2}{\sigma_g^2} \right] + \eta_y P_{opt_total} \frac{1}{\sigma_y\sqrt{2\pi}} \exp \left[-0.5 * \frac{(\lambda - \lambda_{peak_y})^2}{\sigma_y^2} \right] \tag{4}$$

where P_{opt_b} , P_{opt_g} , P_{opt_y} and P_{opt_total} stand for the optical power (W) in each separate spectrum of blue, green, yellow and white. λ_{peak_b} , λ_{peak_g} and λ_{peak_y} in order are the peak wavelengths in the emission spectrum (nm) of each chromatic light. The non-dimensional ratios of chromatic lights spectra to the spectrum of white light, are expressed respectively as η_b , η_g and η_y . σ_b , σ_g and σ_y in turn are the coefficient of FWHM (nm) for the wavelength ranges of chromatic lights. Thus, this extended Gaussian model involving three chromatic spectra is the standard model to compute the SPD of WLED with phosphor coating. In Figure 6 is luminous flux corresponding to different concentration levels of green and red phosphor. The sharp increase in lumen output occurs as the concentration of green phosphor $\text{NaYF}_4:\text{Er}^{3+}$, Yb^{3+} grows from 2% wt to 20% wt is shown in Figure 6. In contrast, increasing value of concentration, 2-20% wt., red-emitting phosphor has caused the lumen output to decrease dramatically which can be explained by applying Beer's law. $\alpha\text{-SrO}\cdot 3\text{B}_2\text{O}_3:\text{Sm}^{2+}$ concentration induces reduction factor μ_{ext} growth while being detrimental to the light transmission power. Thus, when the thickness of the phosphor layers is constants, the lumen output of WLEDs can be degraded in accordance to the growth of $\alpha\text{-SrO}\cdot 3\text{B}_2\text{O}_3:\text{Sm}^{2+}$ concentration. However, taking into accounts the benefits of red phosphor $\alpha\text{-SrO}\cdot 3\text{B}_2\text{O}_3:\text{Sm}^{2+}$ particles to the color quality of WLEDs as expressed through color rendering index, color quality scale, and higher luminous efficiency of double-layer phosphor with $\alpha\text{-SrO}\cdot 3\text{B}_2\text{O}_3:\text{Sm}^{2+}$ in comparison with single layer structure without $\alpha\text{-SrO}\cdot 3\text{B}_2\text{O}_3:\text{Sm}^{2+}$, this reduction fades into insignificance. Therefore, it depends on the intention of manufacturers to determine the most appropriate $\alpha\text{-SrO}\cdot 3\text{B}_2\text{O}_3:\text{Sm}^{2+}$ concentration in WLEDs mass-production.

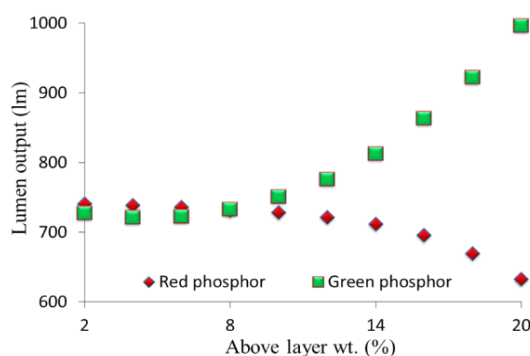


Figure 6. The luminous flux in connection with the variation of $\text{NaYF}_4:\text{Er}^{3+}$, Yb^{3+} and $\alpha\text{-SrO}\cdot 3\text{B}_2\text{O}_3:\text{Sm}^{2+}$ phosphors' concentration

4. CONCLUSION

In the article, the influences of green $\text{NaYF}_4:\text{Er}^{3+}$, Yb^{3+} and red $\alpha\text{-SrO}\cdot 3\text{B}_2\text{O}_3:\text{Sm}^{2+}$ phosphor on optical properties of remote structure with two phosphor layers have been studied and clearly demonstrated. By applying the Gaussian model, the advantage of $\alpha\text{-SrO}\cdot 3\text{B}_2\text{O}_3:\text{Sm}^{2+}$ application is affirmed and this phosphor is considered the most appropriate material to enhance the color quality of WLEDs. In addition, $\text{NaYF}_4:\text{Er}^{3+}$, Yb^{3+} is the phosphor chosen for better the luminous efficiency of WLEDs. These two phosphors are not only suitable for low but also for high color temperature WLEDs. With these results, this study has accomplished the purpose of white light color quality enhancement though this is one of the hardest goals for remote-phosphor design. Nevertheless, it still presents a minor disadvantage in luminous flux. As the concentrations of $\text{NaYF}_4:\text{Er}^{3+}$, Yb^{3+} or $\alpha\text{-SrO}\cdot 3\text{B}_2\text{O}_3:\text{Sm}^{2+}$ is exceeded, the color quality or luminous flux is noticeably decreased. This problem has proven the importance of the appropriate selection for phosphor concentrations, depending on the goal of the manufacturer. This research paper is also become an essential reference in the field of fabricating high-quality WLEDs.

REFERENCES

- [1] Trang T. T., et al., "Improving luminous flux and color homogeneity of dual-layer phosphor structure," *Telecommunication Computing Electronics and Control*, vol. 17, no. 5, pp. 2643-2649, October 2019.
- [2] Li J. S., Tang Y., Li Z. T., Rao L. S., Ding X. R., Yu B. H., "High efficiency solid-liquid hybrid-state quantum dot light-emitting diodes," *Photonics Research*, vol. 16, no. 12, pp. 1107-1115, December 2018.
- [3] Zhang A., Wang B., Yan Q., Wang Y. C., Jia J., Jia H., Xu B. S., Wong W. Y., "Tunable white light emission of a large area film-forming macromolecular complex with a high color rendering index.," *Optical Materials Express*, vol. 8, no. 12, pp. 3635-3652, December 2018.
- [4] Yanru Tang Y. R., et al., "Composite phase ceramic phosphor of $\text{Al}_2\text{O}_3\text{-Ce: YAG}$ for high efficiency light emitting," *Optics Express*, vol. 23, no. 14, pp. 17923-17928, July 2015.

- [5] Peng Y., *et al.*, "Optical performance improvement of phosphor-in-glass based white light-emitting diodes through optimized packaging structure," *Applied Optics*, vol. 55, no. 29, pp. 8189-8195, October 2016.
- [6] Ran Ma R., *et al.*, "Energy transfer properties and enhanced color rendering index of chromaticity tunable green-yellow-red-emitting $Y_3Al_5O_{12}:Ce^{3+}, Cr^{3+}$ phosphors for white light-emitting diodes," *Optical Materials Express*, vol. 7, no. 2, pp. 454-467, January 2017.
- [7] He G. X., Tang J., "Study on the correlations between color rendering indices and the spectral power distributions: comment," *Optics Express*, vol. 23, no. 3, February 2015.
- [8] Shi H. L., *et al.*, "Luminescence properties of YAG:Ce, Gd phosphors synthesized under vacuum condition and their white LED performances," *Optical Materials Express*, vol. 4, no. 4, pp/ 649-655, April 2014.
- [9] Huang C. H., *et al.*, "Thermally stable green $Ba_3Y(PO_4)_3:Ce^{3+}, Tb^{3+}$ and red $Ca_3Y(AlO)_3(BO_3)_4:Eu^{3+}$ phosphors for white-light fluorescent lamps," *Optics Express*, vol. 19, no. S1, pp. A1-A6, January 2011.
- [10] Zhang G., Ding K., He G., Zhong P., "Spectral optimization of color temperature tunable white LEDs with red LEDs instead of phosphor for an excellent IES color fidelity index," *OSA Continuum*, vol. 2, no. 4, pp. 1056-1064, April 2019.
- [11] Wang B., *et al.*, " Eu^{3+} doped high-brightness fluorophosphate laser-driven glass phosphor," *Optical Materials Express*, vol. 9, no. 4, pp. 1749-1762, April 2019.
- [12] Wang M. T., Huang J. M., "Accurate control of chromaticity and spectra by feedback phosphor-coating," *Optics Express*, vol. 23, no. 9, pp. 11576-11585, May 2015.
- [13] Kim S. N., Iqbal F., Kim H. S., "Relationship between phosphor properties and chromaticity of phosphor-in-glass," *Applied Optics*, vol.56, no. 34, pp. 9477-9483, December 2017.
- [14] Zhang Z. J., Yang W. C., "Tunable photoluminescence in $Ba_{1-x}Sr_xSi_3O_4N_2: Eu^{2+}/ Ce^{3+}, Li^+$ solid solution phosphors induced by linear structural evolution," *Optical Materials Express*, vol. 9, no.4, pp. 1922-1932, 2019.
- [15] Dubey A. K., Gupta M., Kumar V., Mehta D. S., "Laser-line-driven phosphor-converted extended white light source with uniform illumination," *Applied Optics*, vol. 58, no. 9, pp. 2402-2407, March 2019.
- [16] Chen M. Z., Wang Q. X., Gu H. R., Tan Q. F., "Diffraction optical element with same diffraction pattern for multicolor light-emitting diodes," *Applied Optics*, vol.55, no. 1, pp. 159-164, February 2016.
- [17] Segawa H., Hirosaki N., "Europium-doped SiAlON and borosilicate glass composites for white light-emitting diode," *Applied Optics*, vol. 54, no. 29, pp. 8727-8730, October 2015.
- [18] Cheng J., *et al.*, "Synthesis and photoluminescence properties of $Sr_4La(PO_4)_3O:RE^{3+}(RE=Eu/Tb/Ce)$ phosphors," *Chinese Optics Letters*, vol. 15, no. 12, December 2017.
- [19] Cantore M., *et al.*, "High luminous flux from single crystal phosphor-converted laser-based white lighting system," *Optics Express*, vol. 24, no. 2, pp. A215-A221, January 2016.
- [20] Jeon S. W., *et al.*, "Improvement of phosphor modeling based on the absorption of Stokes shifted light by a phosphor," *Optics Express*, vol. 22, no. S5, pp. A1237-A1242, August 2014.
- [21] Xu X. G., *et al.*, "High luminescent $Li_2CaSiO_4:Eu^{2+}$ cyan phosphor film for wide color gamut field emission display," *Optics Express*, vol. 20, no. 16, pp. 17701-17710, July 2012.
- [22] Hayashida T., *et al.*, "Appropriate indices for color rendition and their recommended values for UHDTV production using white LED lighting," *Optics Express*, vol. 25, no.13, pp. 15010-15027, June 2017.
- [23] Heikkinen V., *et al.*, "Stroboscopic scanning white light interferometry at 2.7 MHz with 1.6 μm coherence length using a non-phosphor LED source," *Optics Express*, vol. 21, no. 5, pp. 5247-5254, March 2013.
- [24] Tsai M. S., *et al.*, "Optical design of tunnel lighting with white light-emitting diodes," *Applied Optics*, vol. 53, no. 29, pp. H114-H120, October 2014.
- [25] Fouliard Q. T., *et al.*, "Modeling luminescence behavior for phosphor thermometry applied to doped thermal barrier coating configurations," *Applied Optics*, vol. 58, no. 13, pp. D68-D75, May 2019.